Translational Oncology 26 (2022) 101562

Contents lists available at ScienceDirect

Translational Oncology

journal homepage: www.elsevier.com/locate/tranon

Original Research

ARNTL2 is an indicator of poor prognosis, promotes epithelial-to-mesenchymal transition and inhibits ferroptosis in lung adenocarcinoma

Huan Zhang [a,b,1], Guangyao Shan [a,b,1], Xing Jin [a,b,1], Xiangyang Yu [c], GuoShu Bi [a,b], Mingxiang Feng [a,b], Hao Wang [a,b], Miao Lin [a,b], Cheng Zhan [a,b], Qun Wang [a,b], Ming Li [a,b,*]

[a] Department of Thoracic Surgery, Zhongshan Hospital, Fudan University, Shanghai, China
[b] Cancer Center, Zhongshan Hospital, Fudan University, Shanghai, China
[c] Department of Thoracic Surgery, Peking Union Medical College, National Cancer Center/National Clinical Research Center for Cancer/Cancer Hospital/Shenzhen Hospital, Chinese Academy of Medical Sciences, Shenzhen, China

ARTICLE INFO

Keywords:
ARNTL2
Lung adenocarcinoma
EMT
Ferroptosis

ABSTRACT

Objectives: ARNTL2, as a circadian transcription factor, has been recently proposed to play an important role in a variety of tumors. however, the role of ARNTL2 in lung carcinogenesis and progression remains unclear. The purpose of this study was to investigate the effect of ARNTL2 on the clinical characteristics and prognosis of lung adenocarcinoma and to explore the relationship between ARNTL2 and EMT, ferroptosis in lung adenocarcinoma.
Methods: The Cancer Genome Atlas (TCGA) database's multi-omics data were downloaded using the Xena browser. Based on the expression levels of ARNTL2, patients with lung adenocarcinoma from TCGA were divided into two groups: those with high ARNTL2 expression and those with low ARNTL2 expression. ARNTL2 was studied for its effects on lung adenocarcinoma's clinicopathological, genomic, and immunological characteristics. Furthermore, *in vivo* and *in vitro* assays were used to confirm the impact of ARNLT2 knockdown on lung adenocarcinoma cells.
Results: We found ARNTL2 is highly expressed in lung adenocarcinoma and was an independent predictor of a poor prognosis in patients with lung adenocarcinoma. In addition, we demonstrated that knockdown of ARNTL2 promoted ferroptosis, inhibited EMT, cell proliferation, migration and invasion in lung adenocarcinoma. In contrast, overexpressing ARNTL2 yielded the opposite results.
Conclusions: ARNTL2 is an independent unfavorable prognostic factor for lung adenocarcinoma. It plays a facilitating *role in* the development of lung adenocarcinoma, especially in promoting EMT and inhibiting ferroptosis, revealing that ARNTL2 may be a potential biomarker for lung adenocarcinoma.

Introduction

In 2020, lung cancer has been the leading cause of cancer death worldwide [1]. The most common subtype is lung adenocarcinoma (LUAD) [2]. Despite efforts and advancements in lung adenocarcinoma therapy, the prognosis of LUAD patients remains bleak; the 5-year survival rate of lung cancer patients was less than 20% [3]. As a result, it is critical to investigate the etiology and mechanisms of LUAD malignant progression to develop more effective treatment strategies.

Circadian rhythms are oscillations that occur every 24 h and can

Abbreviations: LUAD, lung adenocarcinoma; ARNTL2, Aryl Hydrocarbon Receptor Nuclear Translocator Like 2; TMB, tumor mutation burden; TCGA, The Cancer Genome Atlas; AJCC, American Joint Committee on Cancer; DEGs, differentially expressed genes; CNV, copy number variations; miRNAs, microRNAs; GO, Gene Ontology; KEGG, Kyoto Encyclopedia of Genes and Genomes; FDR, false discovery rate; GDSC, the Genomics of Drug Sensitivity in Cancer; IC50, half-maximal inhibitory concentration; shRNAs, short hairpin RNAs; qRT-PCR, Quantitative real-time polymerase chain reaction; TBST, tris-buffered saline Tween-20; MS, Microsatellites; STR, short tandem repeats; SSR, simple sequence repeats; TME, tumor microenvironment; NK cells, Natural killer cells.; ICIs, immune-checkpoint inhibitors; EMT, Epithelial-to-mesenchymal transition.

* Corresponding author at: Department of Thoracic Surgery, Zhongshan Hospital, Fudan University, No. 180, Fenglin Road, Shanghai, China.
E-mail address: li_m14@fudan.edu.cn (M. Li).

[1] These authors contributed equally to this work.

https://doi.org/10.1016/j.tranon.2022.101562
Received 15 April 2022; Received in revised form 17 September 2022; Accepted 5 October 2022

initiate and monitor various biological processes [4]. Circadian rhythms in mammals are controlled by a central clock in the suprachiasmatic nucleus of the anterior hypothalamus and peripheral oscillators found in many peripheral tissues [5]. Many studies have demonstrated that environmental disruptions to the circadian rhythm may increase the risk of certain cancers [6]. A critical circadian transcription factor Aryl Hydrocarbon Receptor Nuclear Translocator Like 2 (ARNTL2), has been shown to participate in the organization of feedback loops to provide near 24 h rhythmicity [7]. It has also been demonstrated to play an essential role in various tumors. ARNTL2 is associated with poor survival and immune infiltration in clear cell renal cell carcinoma [8] and triple-Negative Breast Cancer [9]. Besides, ARNTL2 has also been found to promote metastasis of colon carcinoma [10] and estrogen Receptor-Negative Breast Cancer [11]. However, research on the role of ARNTL2 in lung adenocarcinoma is scarce and insufficiently thorough. In our study, we first found that ARNTL2 promoted EMT and inhibited ferroptosis in LUAD cells.

The current study analyzed 513 lung adenocarcinoma samples from the Cancer Genome Atlas (TCGA) database; we discovered that ARNTL2 is highly expressed in lung adenocarcinoma and has a negative impact on LUAD patient's prognosis. Furthermore, ARNTL2 expression was found to significantly impact the progression and immune microenvironment of lung adenocarcinoma. Through *in vivo* and *in vitro* experiments, we also confirmed that ARNTL2 promotes the proliferation, migration, and invasion of lung adenocarcinoma cells. The findings suggest that ARNTL2 plays a vital role in developing, progressing, and treating lung cancer, laying the groundwork for future mechanistic research and treatment.

Methods

Data processing

Gene expression data of LUAD patients (FPKM normalized) and corresponding clinical and survival information of The Cancer Genome Atlas (TCGA) were downloaded from the UCSC Xena browser (GDC hub: https://gdc.xenahubs.net) [12]. The data with missing prognosis information, including outcome status and survival time, was removed. The edition of lung cancer staging was classified according to the American Joint Committee on Cancer (AJCC) TNM Classification for Lung and Pleural Tumors (eighth edition).

TIMER analysis

The "DiffExp" module in TIMER [1] web server [13] was applied in examining the expression level and matched non-carcinoma tissues in LUAD tumors.

Genome statistical analysis

Based on the median values of ARNTL2 expression level, TCGA cases were divided into high and low groups. The following genome statistical analyses were carried out in R version 4.0.3:

(a) **Differentially expressed genes (DEGs):** DEGs and miRNAs were identified using the limma package. To calculate DEGs and miRNA expression changes, the moderated *t*-test was used. The Benjamini and Hochberg method was used to adjust the *P-value* as FDR. The adjusted *P-value* $\langle$ 0.05, and the log fold change $\rangle$ 0.5 [14].

(b) **Copy number variations (CNV) and microRNAs (miRNAs):** the maftools package was used to compare the distribution of somatic mutations and the types of CNV [15]. The significance of the mutational frequency was determined using an adjusted *P-value* $<$ 0.01. The Kruskal-Wallis test was used to compare the somatic mutations and types of copy number variations between the high and low-ARNTL2 groups, and an adjusted *P-value* $<$0.05 was considered statistically significant. The oncoplot function was used to display the results.

(c) **GO and KEGG:** The clusterProfiler R package was used to perform GO, and KEGG pathway enrichment analysis on the DEGs' involved pathways and biological functions [14]. The cut-off values were determined to be adjusted P $<$ 0.05 and false discovery rate (FDR) $<$ 0.05.

(d) **Ferroptosis analysis:** Ferroptosis-related genes are derived from Ze-Xian Liu et al.'s systematic analysis of Ferroptosis's aberrances and functional implications in Cancer [16].

(e) **mRNAi analysis:** To calculate mRNAsi, we use the OCLR algorithm developed by Malta et al. [17]. The gene expression profile contains 11,774 genes based on mRNA expression characteristics. We used the same Spearman correlation (RNA expression data), subtracted the minimum value, and divided it by the maximum value's linear transformation, which maps the dryness index to the range [0, 1].

(f) **Drug sensitivity analysis:** Using the largest publicly available pharmacogenomics database [the Genomics of Drug Sensitivity in Cancer (GDSC), https://www.cancerrxgene.org/], we predicted the chemotherapeutic response for each sample. The R package "pRRophetic" was used to implement the prediction process, in which the samples' half-maximal inhibitory concentration (IC_{50}) was estimated using ridge regression, and the prediction accuracy was calculated. The default values were used to set all parameters after removing the batch effect of combat and tissue type from allSoldTumours, and duplicate gene expression was summarised as a mean value [18].

(g) **Immune infiltration and immune checkpoints:** To estimate immune infiltration, we used the QUANTISEQ method from the Immunodeconv R package [19]. SIGLEC15, TIGIT, CD274, HAVCR2, PDCD1, CTLA4, LAG3, and PDCD1LG2 were chosen as immune-checkpoint-relevant transcripts and their expression levels were determined. Based on the RNA-seq expression profiles, the QUANTISEQ method (https://quantuseq.stanford.edu) [20] was chosen to analyze the relative levels of the ten tumor-infiltrating immune cell phenotypes. The distribution of ten tumor-infiltrating immune cell types between poor and good prognostic signatures was studied.

(h) **Correlation analysis of ARNTL2 expression and TMB** [21,22]: We used Spearman's correlation analysis to describe the correlation between quantitative variables that did not have a normal distribution. The Pearson correlation coefficient has a value range of [-1,1]. A higher absolute value indicates a stronger association, and the sign indicates whether the two variables are associated positively or negatively. The density curve on the right represents the TMB score, while the upper-density curve represents the gene's distribution trend.

The R foundation implemented all aforementioned analysis methods and the R package for statistical computing (2020) version 4.0.3.

Single-cell analysis

Single-cell analysis was performed through the CANCERSEA website. CancerSEA is the first dedicated database that comprehensively decodes distinct functional states of cancer cells at single-cell resolution [23].

Prognosis analysis

Prognostic information was analyzed in the PrognoScan and Kaplan–Meier plotter database [24].

Cell culture and lentivirus infection

Lung adenocarcinoma cell lines (A549 and H1299) were purchased from the Chinese Academy of Sciences Cell Bank. Cells were cultured in DMEM (Hyclone, Logan, UT, USA) supplemented with 10% fetal bovine serum (Hyclone), 100 U/mL penicillin, and 100 U/mL streptomycins in a humidified 5% CO2 atmosphere at 37 °C.

Two different short hairpin RNAs (shRNAs) encoding shARNTL2 and scramble shRNA control (catalog) was designed by Shanghai Genechem Co., Ltd, and cloned into a lentivirus vector with puromycin resistance, which was then transfected into cells and screened with puromycin to ensure transfection efficacy. Viral transduction was performed as the manufacturer's protocol. After three days of virus transfection, knockdown was verified by western blot analysis using ARNTL2-specific antibody (ab221557, Abcam). Sequences of the shRNAs and the control are provided in Supplementary Table 1.

Compounds

The following compounds were obtained from Topscience (USA): RSL3 (T3646), cisplatin (T1564). RSL3 was dissolved in PBS (Beyotime, Shanghai, China) and cisplatin in DMSO (Beyotime), according to their solubility, and then stored at −20 °C.

Western blot

RIPA buffer (Beyotime, Shanghai, China) containing protease and phosphatase inhibitors cocktail (Beyotime) were used to extract proteins, enhanced BCA Protein Assay Kit (Beyotime) was used for protein quantification. As previously reported [25], Protein samples were separated by electrophoresis on SDS-PAGE and transferred to a polyvinylidene difluoride membrane (Merck-Millipore, Burlington, MA, USA). After the transfer, the blots were blocked with 5% milk for 1 h and incubated with primary antibody for 12 h at 4 °C. Then, tris-buffered saline Tween-20 (TBST) was used to wash the membranes three times. After washing, the membranes were incubated with secondary antibodies at room temperature for one hour. Finally, the protein bands were visualized and analyzed using a Moon Chemiluminescence Reagent kit (Beyotime). Three biological replicates were analyzed and western blots repeated three times. The following antibodies were used in this study: Anti-ANRTL2 antibody (1:1000, Abcam, ab221557), Anti-E-Cadherin antibody (1:1000, Cell Signaling Technology, #9782), Anti-N-Cadherin antibody (1:1000, Cell Signaling Technology, #9782), Anti-β-catenin antibody (1:1000, Cell Signaling Technology, #9782), Anti-Vimentin antibody (1:1000, Cell Signaling Technology, #9782), Anti-Snail antibody (1:1000, Cell Signaling Technology, #9782), Anti-Fibronectin (1:1000, Abcam, ab2413), Anti-NFE2L2 antibody (1:1000, Cell Signaling Technology, #12,721), Anti-GLS2 antibody (1:1000, abcam, ab113509), Anti-SLC7A11 antibody (1:1000, Cell Signaling Technology, #98,051), Anti-CISD1 antibody (1:1000, Cell Signaling Technology, #83,775), and Anti-β-Actin antibody (1:1000, Beyotime, AF0003) .

Cell viability assays

For cell proliferation assays, cells were seeded in quintuplicate into black 96-well plates at a density of 2000 cells per well at logarithmic growth phase. After incubation at 37 °C for 0, 24, 48, 72, 96, and 120 h. For cytotoxicity assays, 5000 cells per well were seeded in quintuplicate in 96-well plates and incubated for 24 h. Cells were treated with different doses of chemotherapy drugs for specific times as needed. the cell proliferation was measured by Enhanced Cell Counting Kit-8 Viability Assay Kit (Beyotime) according to the manufacturer's protocol.

Wound healing assay

Control shRNA and shARNTL2 cells were inoculated on the 6-well plate on average. Cells were grown into monolayer and manual scratching with a 200 μl pipette tip. Cells were rinsed with PBS and incubated at 37 °C in serum-free media. Photographs of the wounded areas were taken every 24 h by phase-contrast microscopy.

Transwell migration and invasion assay

Cell migration and invasion abilities were measured by Transwell assays using the 24-well transwell chambers with 8 μm polycarbonate membranes (Corning, NY). The uncoated were used to determine migration, and pre-coated with Matrigel Basement Membrane Matrix were used to determine invasion (BD Biosciences). The chambers were rehydrated in a serum-free medium for 2 h as described by the manufacturer. Then the upper chambers were added with serum-free medium, while the lower chambers were added with serum medium. Cells were seeded onto the upper chambers with a density of 5×104 cells per well and incubated for 24 h at 37 °C, 5% CO2. Cells migrated toward the lower chambers were fixed with methanol and stained with 0.5% crystal violet. Each assay was photographed under the inverted microscope (Olympus), and the number of cells within each chamber was counted by ImageJ software.

Clone formation assay

Control or ARNTL2 shRNA-transduced A549 and H1299 cells (3 × 103 cells/well) were cultured in 6-well plates were cultured at 37 °C in 5% CO2 environment. ARNTL2 shRNA-transduced or control cells were seeded in 6-well plates at a density of 5 × 106 cells per well and cultured at 37 °C in 5% CO2 environment. After nine days, cells were stained with 4% formaldehyde/0.005% gentian violet solution and captured under the inverted microscope.

Immunohistochemistry and immunofluorescence

The tissue specimens were collected from both tumor and adjacent normal tissues of 100 patients with LUAD who received surgery from September to November 2020 in the Zhongshan Hospital. As previously reported [26], the tissues were stained by a GTVision + Detection System/Mo&Rb Immunohistochemistry kit (GK500710, GeneTech, Shanghai, China) following the manufacturer's protocol. Specifically, the 5-μm paraffin-embedded tissues were dewaxed, rehydrated, and incubated with antibodies against ARNTL2 (1:500, Abcam, Cambridge, UK) at 4 °C overnight, and then were incubated with biotinylated secondary antibodies. For immunofluorescence, sections were incubated with primary antibodies against ARNTL2 (rabbit polyclonal, 1:500), followed by incubation with the respective secondary antibodies (Cy3-labeled goat anti-rabbit IgG). DAPI nuclear counterstaining was then performed. Finally, a fluorescence microscope was used to take micrographs.

Subcutaneous tumor formation

Female BALB/c nude mice (4 weeks old) were obtained from GemPharmatech Co., Ltd, (Jiangsu, China) and housed and maintained in laminar airflow cabinets under specific pathogen-free conditions. For the subcutaneous A549 tumor model, 1×10 [6] A549 cells (Group 1, sh-control; Group 2, sh1-ARNTL2) were injected subcutaneously into the right flank of each mouse (8/group). In life, mice were monitored regularly, and tumors were measured with vernier calipers every 5 days (tumor volume was calculated as π/6 × length × width × width). The mice were euthanized after 6 weeks, and tumors were isolated and weighed for further analyses.

Statistical analysis

All experiments were performed in at least triplicates. Statistical analyses in the current study were completed by R version 3.6.1 (R Foundation for Statistical Computing, Vienna, Austria). The R package included survival, rms, ggplot2, limma, maftools, clusterProfiler, and Immunodeconv. Statistical significance was set at a two-sided *P-value* < 0.05. Categorical variables were compared using Fisher's exact test. Pearson's c2 test and continuous variables were compared using Student's *t*-test and the Wilcoxon test. Multivariable Cox regression analyses were used to test independent prognostic value using the R package survival and the coxph function. Image analysis was performed using ImageJ software.

Result

Gene expression and clinical features

An earlier study discovered that ARNTL2 was frequently overexpressed in various cancers [27]. Fig. 1A depicts the differential expression of ARNTL2 between tumor and adjacent normal tissues in TCGA. To further validate whether ARNTL2 was differentially expressed in lung adenocarcinoma tissues, 513 cases of LUAD patients' data from TCGA database were analyzed, and ARNTL2 expression in LUAD tissues was significantly higher than in normal adjacent tissues (P < 0.001). A similar conclusion was reached after combining GTEx data (Fig. 1B). Furthermore, we divided LUAD patients in TCGA database into two equal groups based on ARNTL2 expression. Significant differences in baseline characteristics were found between the two groups, as shown in Table 1 and Supplementary Fig. 1. Patients in the high-ARNTL2 group were more likely to be male and had more advanced N and AJCC stages.

Survival analysis

The TCGA database was used to examine the prognosis of LUAD patients. We discovered that high ARNTL2 expression predicted poor survival, as shown in Fig. 1C: OS: HR= 1.53 (95% CI: 1.14–2.05), p = 0.005; PFS: HR= 1.35 (95% CI: 1.03–1.78), p = 0.031. These patients were also subjected to univariate and multivariate analyses to validate survival factors. ARNTL2 (p < 0.001), T stage (p < 0.001), and N stage (p < 0.001) were found to be statistically significant predictors of tumor-specific survival in univariate analyses. ARNTL2 (p < 0.001), T stage (p = 0.005), and N stage (p = 0.001) remained independent prognostic predictors for LUAD patients in multivariate analysis. The forest plot below depicts the relationships between survival outcomes and parameters (Fig. 1D).

TMB and mRNAsi analyses

Tumor mutation burden (TMB) has gotten a lot of attention as one of the immunotherapy biomarkers in recent years [28]. Using the TCGA database, we investigated the relationship between ARNTL2 gene expression and TMB in LUAD patients. A positive correlation was discovered between ARNTL2 and TMB (Fig. 1E); thus, the expression level of ARNTL2 may serve as a reference value for immunotherapy.

It has been reported that mRNAsi is a reliable method for determining the degree of tumor differentiation [29]. The higher mRNAsi values are associated with a higher degree of tumor dedifferentiation and a worse prognosis. As depicted in Fig. 1F, the mRNAsi in LUAD tumor specimens was significantly higher than in normal lung tissue. Furthermore, compared to the low ARNTL2 expression group, the mRNAsi in the high ARNTL2 group was significantly higher, which may be linked to the poor prognosis of patients in the high ARNTL2 group.

Somatic mutations

According to previous research, the number of somatic mutations may be related to tumor development [30]. Fig. 1G depicts the distribution of somatic mutations in the high-ARNTL2 and low-ARNTL2 groups, indicating that TP53 had a high mutation rate in the high-ARNTL2 group (55% vs. 41%, P-value < 0.01). In contrast, some significant genes, such as RELN (11% in the low subgroup and 18% in the high subgroup), had a lower mutation rate in the high ARNTL2 group.

DEG, GO, KEGG analyses, and single-cell analysis

The prognosis of lung adenocarcinoma patients with varying levels of ARNTL2 expression could be linked to differentially expressed genes (DEGs). So, we analyzed DEG expression to derive a landscape of biological differences (Fig. 2A), and 185 significant different genes were discovered, including 114 upregulated genes in the high-ARNTL2 group, such as SLC2A1, CD109, and ADGRF4 (adjusted P < 0.01), and 71 downregulated genes, such as C16orf89, IRX5, and IRX3 (Supplementary Table 2). The functional enrichment of GO and KEGG in the 185 DEGs was investigated further. Following pathways were linked to the high-ARNTL2 expression: cell cycle, apoptosis, the IL-17 signaling pathway, and the p53 signaling pathway (Fig. 2B). These results were consistent with previous studies [31], which revealed that ARNTL2 is enriched for gene sets associated with LUAD pathogenesis, such as the 'p53 signaling pathway' and cell cycle. Furthermore, we used the CancerSEA database to perform a single-cell analysis of lung adenocarcinoma cells, revealing that ARNTL2 gene expression was highly correlated with epithelial-to-mesenchymal transition (EMT), angiogenesis, and metastasis (Fig. 2C, Supplementary Table 3).

IHC and immunofluorescence: ARNTL2 is highly expressed in lung adenocarcinoma tissues and is associated with poor prognosis

The results of immunohistochemistry confirmed the increased expression of ARNTL2 in lung adenocarcinoma. ARNTL2 overexpression was observed in resected tumor tissues compared to adjacent normal tissues, as manifested in Fig. 3A. Immunofluorescence analyses yielded similar results (Fig. 3B). Furthermore, 120 patients from our institution were divided into high and low groups according to the expression of ARNTL2. Patients with high expression of ARNTL2 had significantly poorer OS (P value = 0.014, Fig. 3C) and PFS (P value = 0.005, Fig. 3C).

ARNTL2 knockdown dramatically inhibites proliferation, invasion, and migration of LUAD cells

To investigate the effect of ARNTL2 on the proliferation and migration of lung adenocarcinoma cells, we created a cell model of ARNTL2 downregulation in A549 and H1299 cells by stably transducing them with ARNTL2 shRNA-expressing lentiviruses. Following that, we used a Western blot to determine the level of ARNTL2 expression after transfection. The knockdown efficiency of shRNA at the protein expression level was confirmed (Fig. 3D). In A549 and H1299 cell lines, ARNTL2 knockdown was very effective. The sh-ARNTL1 and sh-ARNTL2, which exhibited evident knockdown efficacy, were selected for follow-up experiments. Similarly, overexpression of ARNTL2 in A545 and H1299 cells were verified by Western blot analyses (Fig. 3E).

Subsequently, CCK8, clone formation, wound healing, and transwell assays were used to investigate the role of ARNTL2 in tumor proliferation and migration. CCK8 assays revealed that when ARNTL2 was downregulated compared to control cells, the proliferation ability of both A549 and H1299 cells was reduced (Fig. 3F). Clone formation was used to further demonstrate the effect of ARNTL2 on tumor-forming capability in lung adenocarcinoma cells: ARNTL2-knockdown cells formed significantly fewer colonies than control cells (Fig. 3G),

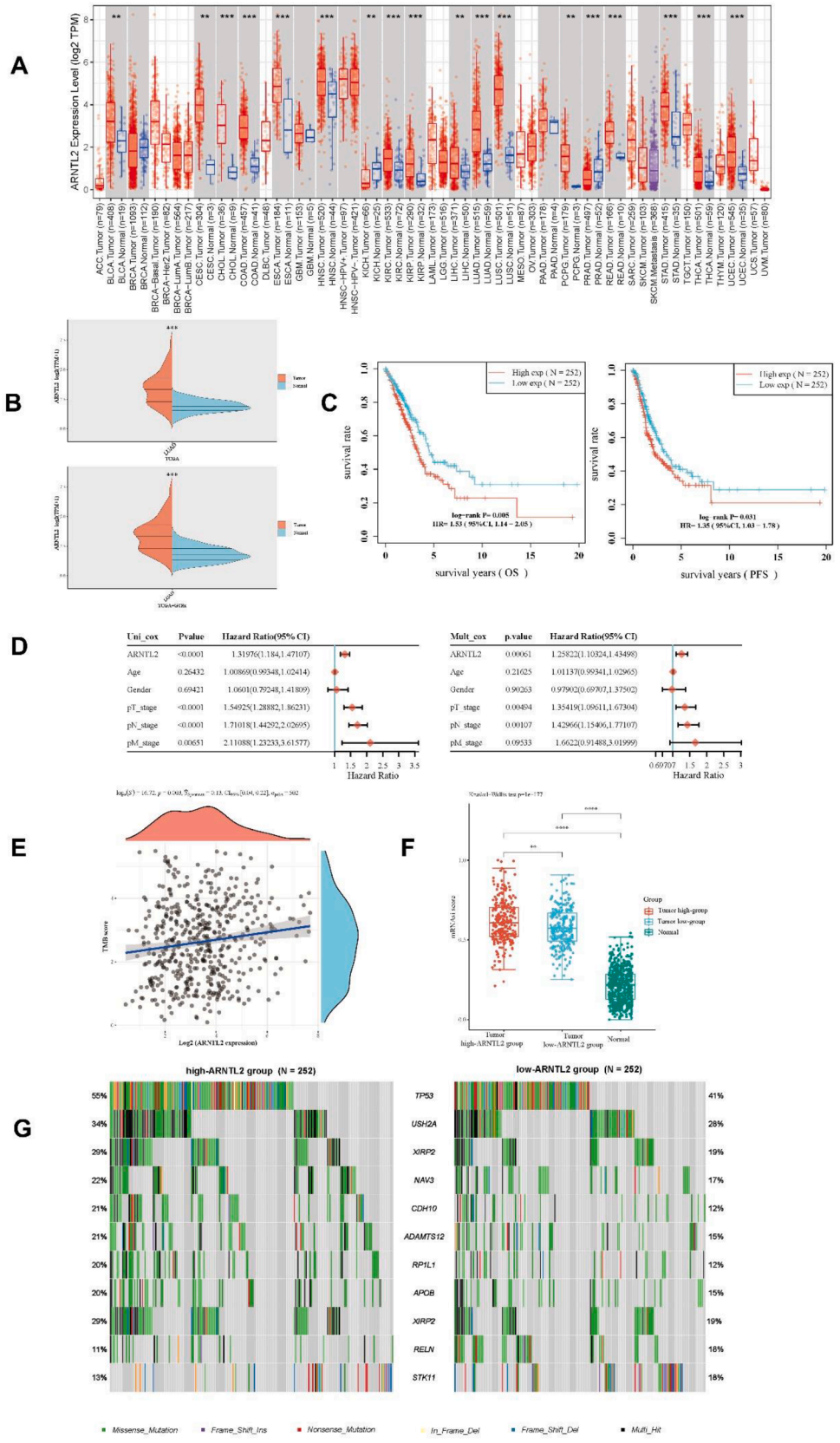

Fig. 1. **A** ARNTL2 expression levels in different tumor types from the TCGA database were determined by TIMER. **B** Differences of ARNTL2 expression in lung adenocarcinoma tissues and normal tissues. **C** Survival curves comparing the high and low expression of ARNTL2 in lung adenocarcinoma. **D** Univariate and multivariate analysis of overall survival in LUAD patients from TCGA database. **E** Scatterplots of correlations between ARNTL2 expression and TMB. **F** The comparison of mRNAsi in high, low ARNTL2 expression groups of lung adenocarcinoma tissues versus normal tissues. **G** Differential mutations and their distributions in the high and low-ARNTL2 expression groups.

Table 1
LUAD patient characteristics according to ARNTL2 expression.

	high- group	low- group	*p value*
Total evaluated	257	256	
Age(years)			0.931
Mean ± SD	65.3 ± 10.3	65.3 ± 9.8	
Sex			0.046
male	130	107	
female	127	149	
Smoking history			0.217
No	34	40	
Yes	213	212	
Unknown	10	4	
Pathologic T stage			0.089
T1	72	96	
T2	142	134	
T3	30	17	
T4	11	8	
Unknown	2	1	
Pathologic N stage			**0.001**
N0	142	188	
N1	60	35	
N2	47	27	
N3	1	1	
Unknown	7	5	
Pathologic M stage			0.099
M0	178	166	
M1	16	9	
Unknown	63	81	
Ajcc 8th stage			**0.001**
1	115	159	
2	69	52	
3	53	31	
4	17	9	
Unknown	3	5	
Radiation			0.781
Yes	7	6	
No/Unknown	250	250	
Chemotherapy			0.350
Yes	82	72	
No/Unknown	175	184	

indicating that ARNTL2 is required for lung adenocarcinoma cell oncogenicity.

The effect of ARNTL2 knockdown on lung adenocarcinoma cell migration and invasion was also confirmed. In a wound-healing assay, ARNTL2-knockdown significantly reduced the migration of A549 and H1299 cells; shControl cells almost recovered the wound within 48 h, but shARNTL2 cells still have large areas of unhealed wounds (Fig. 3H). In the transwell migration and invasion assays, ARNTL2-knockdown cells showed significantly lower infiltration rates than control cells ($p < 0.05$), as shown in Fig. 3I.

Immune infiltration and immune checkpoint analyses

The proportion and composition of immune cells in the tumor microenvironment (TME) significantly impact tumor development and treatment [32]. Corresponding with previous reports [31], we found that CD8+ and CD4+ T cells were found to have significant positive correlations with ARNTL2 expression in lung adenocarcinoma. In contrast, there was a negative correlation between NK cells and Macrophage M2 with ARNTL2 expression (Fig. 4A). Moreover, the high expression of ARNTL2 differed from some vital genes that are closely related to immune checkpoints (Fig. 4B). Compared to the low-ARNTL2 group, tumors with high-ARNTL2 expression had significantly higher levels of CD274, CTLA4, LAG3, and PDCD1. These differences in the immune microenvironment may provide ideas for immunotherapy.

Ferroptosis and drug-sensitive analyses

SLC7A11, CISD1, and other critical genes associated with ferroptosis were found to be overexpressed in the high-ARNTL2 group (Fig. 4C), implying a possible link between ARNTL2 and ferroptosis in lung adenocarcinoma. We knocked down ARNTL2 in A549 and H1299 cell lines and examined the cell viability after 6 h and 24 h exposure to RSL3 with gradient doses, respectively. The results revealed that following ARNTL2 knockdown, LUAD cells became more sensitive to RSL3 treatment (Fig. 4D). In contrast, the opposite results were observed in ARNTL2-overexpressing A549 and H1299 cells. To further verify the effect of ARNTL2 on ferroptosis, we examined the expression levels of several key components involved in ferroptosis pathways after overexpression or knockdown of ARNTL2 in A549 and H1299 cell lines. The results showed that the expression levels of NFE2L2, SLC7A11 and CISD1 were significantly decreased after knockdown of ARNTL2, conversely the expression of GLS2 was increased. The opposite result was obtained after overexpressing ARNTL2 (Fig. 4E).

ANRTL2 expression appears to affect drug sensitivity in lung adenocarcinoma, with IC50s for Cisplatin being significantly lower in the high-ANRTL2 group (Fig. 4F). We knockdown ARNTL2 in A549 and H1299 cell lines and examined the cell viability after 48 h exposure to Cisplatin with gradient doses. The results revealed that knockdown of ARNTL2 significantly desensitized both A549 and H1299 cell lines to Cisplatin. Opposite results were obtained upon ARNTL2 overexpression (Fig. 4G).

ARNTL2 overexpression promotes proliferation, invasion, and migration of LUAD cells

As shown in Fig. 5, the overexpression of ARNTL2 in both A549 and H1299 cell lines generated an opposite effect compared with ARNTL2 knockdown, leading to increased tumor cell proliferation, tumorigenesis, and migration as well as invasion (Fig. 5A, B, and C).

ARNTL2 promotes EMT and Tumor formation of LUAD cells

WB analysis in A549 and H1299 cells confirmed the positive relationship between ARNTL2 and EMT, as shown in Fig. 5D. ARNTL2 knockdown reduced the expression of Snail, Fibronection, vimentin, and N-cadherin in both cell lines while increasing the expression of E-cadherin and β-catenin. Conversely, the opposite result was found in ARNTL2-overexpressing cells, which indicates Overexpression of ARNTL2 promotedEMT while knockdown of ARNTL2 attenuated EMT.

Tumor formation assays were also performed to determine whether ARNTL2 affects tumor growth *in vivo* by subcutaneously injecting ARNTL2 knockdown A549 cells or control cells into the flanks of nude mice. The results showed that ARNTL2 shRNA knockdown significantly inhibited tumor growth in the mouse model: ARNTL2 knockdown resulted in significant shrinkage in all seven mice (Fig. 5E), consistent with *in vitro* results. These findings suggest that ARNTL2 might be an important promoter for lung adenocarcinoma cell growth and invasion, both *in vitro* and *in vivo*.

Discussion

Many studies have recently shown that circadian rhythm disorders may be linked to the development of various cancers in humans [6,33]. Circadian rhythm disruption can alter the expression of several genes, resulting in dysregulated cell proliferation and subsequent tumorigenesis. There is bidirectional coupling between cell cycle and rhythm genes; several cell cycle genes, including c-Myc, Wee1, cyclin D, and p21, have been reported to be affected by the biological clock [34]. For example, BMAL1, one of the core genes of biological rhythm, can indirectly regulate p21 transcription by regulating REV-ERBα/β and RORα/γ. CLOCK/BMAL1 also controls the rhythmic expression of WEE1 kinase, which inhibits the G2/M transition by phosphorylating CDK1 [35]. Furthermore, the circadian clock strongly influences DNA repair, particularly nucleotide excision repair. One of the repair factors, XPA, is regulated by cryptochrome, a common core circadian clock protein

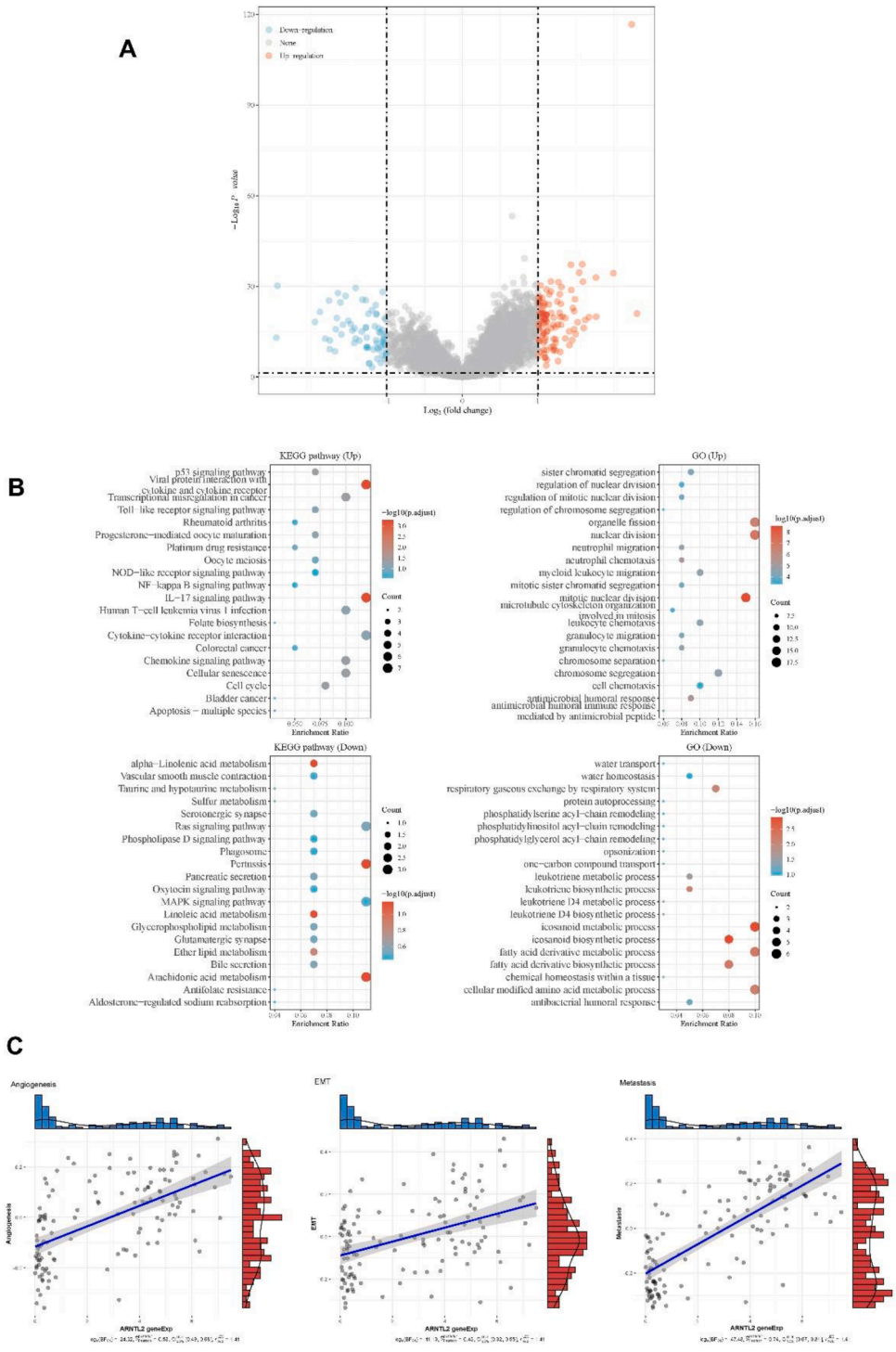

Fig. 2. **A** Differential expressed genes between high and low-ARNTL2 expression groups were shown in a volcano plot. **B** Dot plot of GO and KEGG pathway analysis to the DEGs. **C** Scatterplots of correlations between ARNTL2 expression and angiogenesis, EMT, and Metastasis by single-cell analysis of lung adenocarcinoma cells through the CancerSEA database.

[36]. Another core clock factor, Per1, controls DNA damage-induced apoptosis by interacting with the checkpoint proteins ATM and Chk2 [37].

ARNTL2, also known as BMAL2, is a paralog of BMAL1 and can dimerize with Clock and induce E-box dependent trans-activation, thereby regulating biological rhythms36 and inhibiting periodic genes (Per1, Per2) and cryptochrome genes (Cry1 and Cry2) [38]. ARNTL2 has recently been linked to an oncogenic role in various human cancers. However, there has been little research into the role and mechanism of ARNTL2 in lung adenocarcinoma. We discovered and validated the role of ARNTL2 in the development, progression, and treatment of LUAD by combining TCGA and GTEx data.

ARNTL2 significantly impacts patients' clinical features and outcomes with lung adenocarcinoma. The expression of ARNTL2 was higher in LUAD, as demonstrated in our study. ARNTL2 has also been found to be upregulated in BLCA, BRCA, COAD, and READ [39]. We discovered that high ARNTL2 expression was associated with lymph node metastasis in patients with lung adenocarcinoma; similar findings

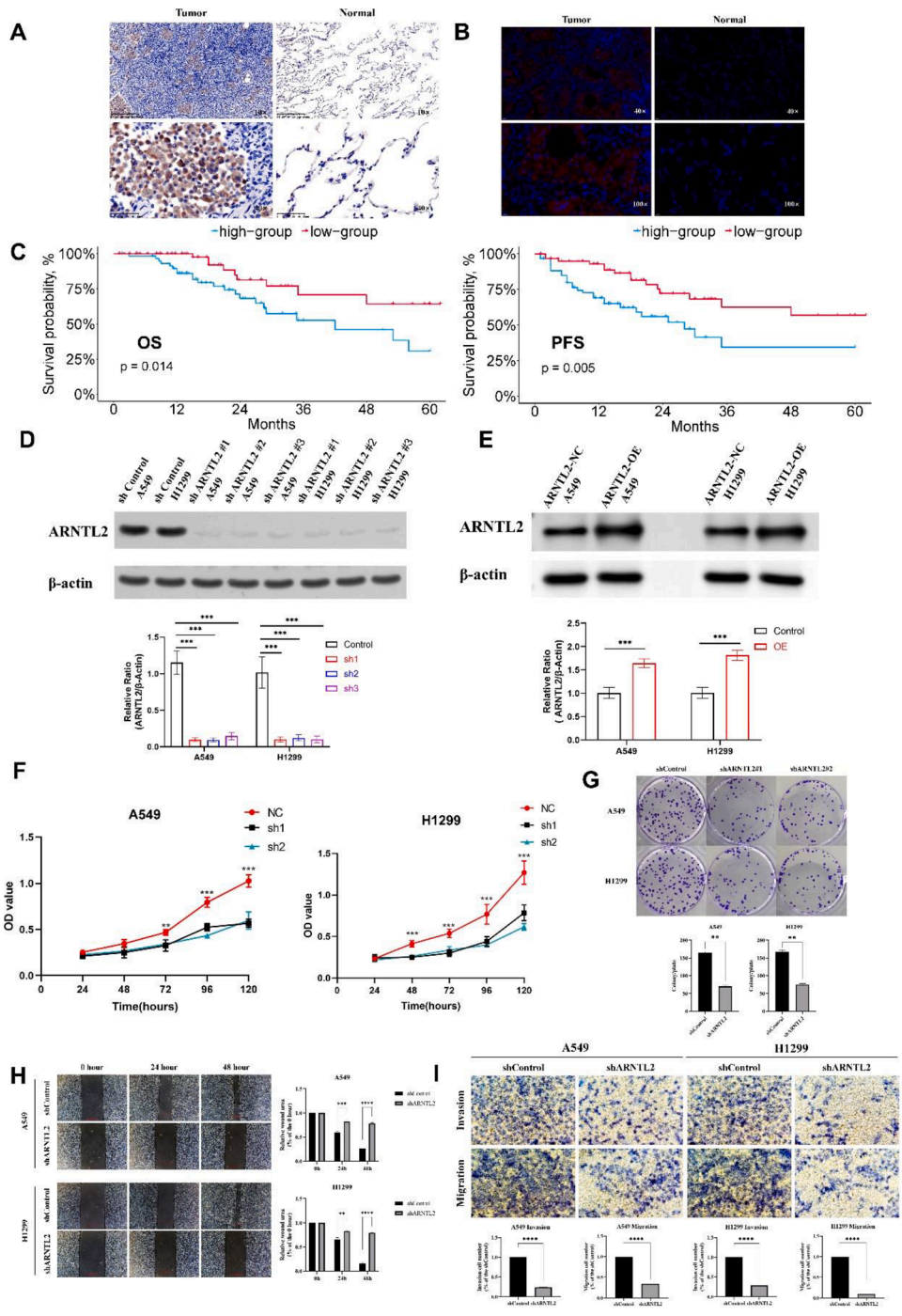

Fig. 3. A-B The IHC (A) and immunofluorescence (B) staining of ARNTL2 in LUAD tissue versus adjacent normal tissues: ARNTL2 expression in tumor tissues was significantly higher than that in adjacent normal tissues. **C** Kaplan-Meier curves of overall survival and progression-free survival according to immunohistochemical staining of the ARNTL2 in patients from our institution. **D-E** Western blotting analyses verifying the ARNTL2 knockdown and overexpression efficiency, quantification was performed by ImageJ: ARNTL2 knockdown was very efficient. **F** The effects of ARNTL2 knockdown on cell proliferation in A549 and H1299 cells through CCK8 assays: knockdown of ARNTL2 dramatically inhibited LUAD cells proliferation. **G** Comparison of colony formation efficiency between ARNTL2-knockdown group and control group: knockdown of ARNTL2 dramatically inhibited colony formation of LUAD cells. **H** Comparison of Wound-healing assays between ARNTL2-knockdown and control groups: ARNTL2 knockdown decreases cell migration in LUAD cells compared to control cells. **I** The invasion and migration capability of LUAD cells transfected with NC or sh-ARNTL2 was analyzed by transwell assay: ARNTL2 knockdown diminished the migration and invasion ability of LUAD cells.

have been reported in colorectal cancer [40]. Furthermore, patients with LUAD with high-ARNTL2 expression had a worse prognosis; thus, the high-ARNTL2 expression could be an independent predictor of prognosis in lung adenocarcinoma.

We confirmed that ARNTL2 promoted LUAD cell proliferation, migration, and invasion using *in vivo* and *in vitro* functional experiments. The mechanism is most likely multifactorial. Our single-cell analysis revealed that ARNTL2 expression was positively associated with EMT and metastasis, confirmed by a Western blot of important EMT marker proteins. A previous study demonstrated that downregulation of ARNTL2 in colon carcinoma could suppress tumor cell proliferation and migration via SMOC2-EMT by inactivation of the PI3K/AKT signaling pathway [10]. Brady et al. also discovered that ARNTL2 works with Clock, another circadian gene, to drive the expression of a complex pro-metastatic secretome that promotes lung adenocarcinoma cell metastasis and growth [41]. Our results also demonstrated, ARNTL2 can inhibit ferroptosis of LUAD cells. And LUAD cells with varied ARNTL2 levels (NC, ARNTL2-knockdown, and ARNTL2-overexpression) showed significant expressing difference in some key ferroptosis-related genes, such as NFE2L2, SLC7A11, and CISD1.

Immunotherapy is gaining popularity in lung cancer treatment. Tumor immune infiltration, and immune checkpoints were all associated with ARNTL2 expression levels in lung adenocarcinoma, indicating ARNTL2 may affect the tumor immune microenvironment of lung adenocarcinoma. For example, ARNTL2 expression was strongly positively correlated with CD8+ T cells but strongly negatively correlated with Natural killer (NK) cells. We also discovered significant differences in the expression of immune checkpoints between patients in the high-

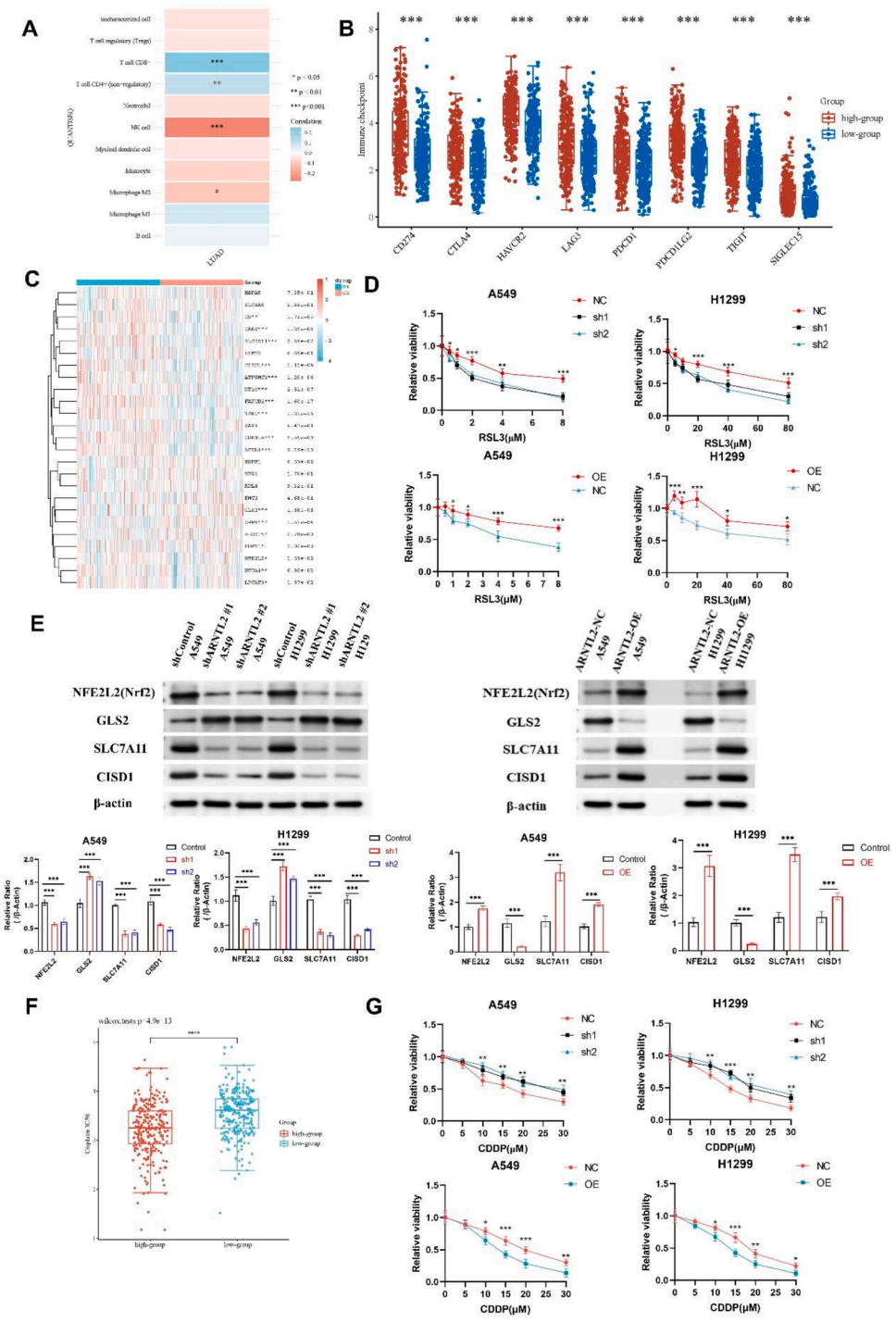

Fig. 4. **A** Correlation of ARNTL2 expression with immune infiltration level in LUAD through QUANTISEQ method. **B** Differences in some important immune genes' expression are closely related to immune checkpoints between high and low-ARNTL2 groups. **C** Differences in the expression of important genes associated with ferroptosis between high and low-ARNTL2 groups. **D** Viability of A549/ H1299 cells upon treatment with ferroptosis inducer, RSL3, at the indicated concentrations for 6 h/ 48 h. **E** The expression of some key genes related to ferroptosis after knockdown or overexpression of ARNTL2 in A549 and H1299 cells. **F** Relationship between drug sensitivity to cisplatin in lung adenocarcinoma and ANRTL2 expression were shown in box plot. **G** Dose-toxicity curves showing the viability of A549 and H1299 cells upon cisplatin treatment at the indicated concentrations for 48 h.

ARNTL2 and low-ARNTL2 groups. More research into the relationship between ARNTL2 and immune checkpoints could be beneficial and necessary.

This study had some limitations as well. Although a large cohort of TCGA and GTEx databases was used to develop and validate the role of ARNTL2 in lung adenocarcinoma, but due to the retrospective nature of our study, design selection bias could not be avoided. Furthermore, this study did not conduct additional in-depth experiments to investigate the mechanism of ARNTL2 promoting tumor development and progression in lung adenocarcinoma, which is the direction of our future research.

Conclusion

ARNTL2 is highly expressed in lung adenocarcinoma and was found to be an independent predictor of a poor prognosis in patients with lung adenocarcinoma. Functional experiments showed that ARNTL2 promoted the cell proliferation, migration, and invasion *in vitro* as well as tumor growth *in vivo*. Notably, we demonstrated for the first time that ARNTL2 promotes EMT and was linked to ferroptosis and cell sensitivity to cisplatin in lung adenocarcinoma cells.

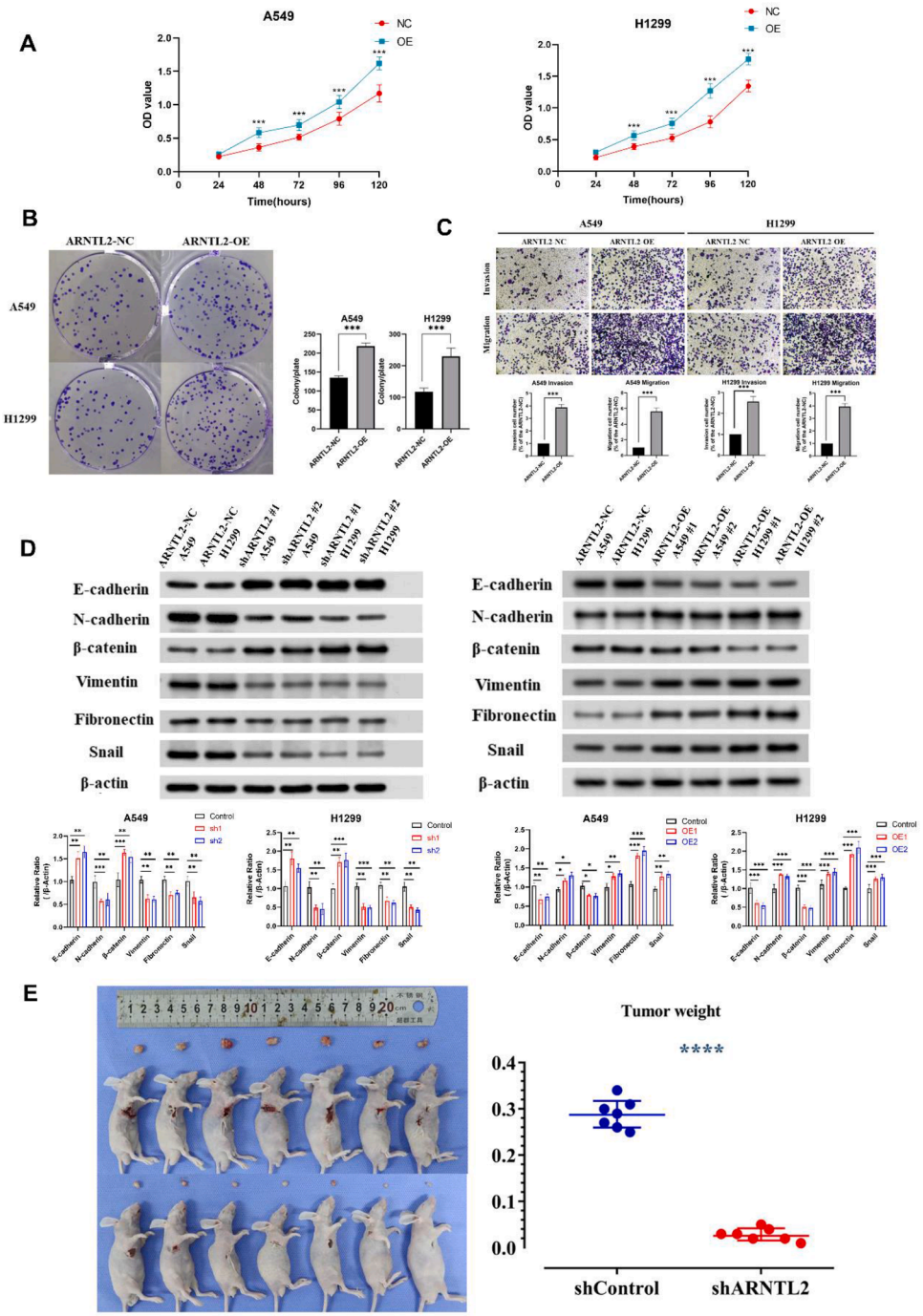

Fig. 5. A-B The effects of ARNTL2 overexpressing on cell proliferation (**A**), and Comparison of colony formation (**B**) in A549 and H1299. **C** The effects of ARNTL2 overexpressing on cell invasion and migration in A549 and H1299 cells. **D** Expressions of EMT-related markers in A549 and H1299 cells with ARNTL2 knockdown and overexpression by WB assays: indicating a positive correlation between ARNTL2 expression and EMT. **E** The effects of ARNTL2 knockdown on tumor growth in mouse xenograft model: ARNTL2 knockdown markedly suppressed xenograft tumor growth of A549 cells.

Formatting of funding sources

This work was supported by the Shanghai Medical Innovation Research Project (Grant No. 20Y11908200), and Research Foundation of Shanghai Municipal Health Commission (20204Y0228).

Ethics approval and consent to participate

All methods were carried out in accordance with relevant guidelines and regulations. All participants signed informed consent according to the ethical requirements in the Declaration of Helsinki. Ethics approved by the ethical committees of Zhongshan Hospital (B2018–137R and Y2020–529).

Consent for publication

Not applicable.

Availability of data and materials

The datasets used and analyzed during the current study are available from the corresponding author on reasonable request.

Disclosures

The authors declare that there is no conflict of interest.

CRediT authorship contribution statement

Huan Zhang: Methodology, Validation, Writing – original draft. **Guangyao Shan:** Visualization, Writing – review & editing, Validation. **Xing Jin:** Methodology, Software. **Xiangyang Yu:** Validation. **GuoShu Bi:** Methodology, Visualization. **Mingxiang Feng:** Visualization. **Hao Wang:** Visualization, Writing – review & editing. **Miao Lin:** Supervision. **Cheng Zhan:** Methodology, Visualization. **Qun Wang:** Data curation, Funding acquisition. **Ming Li:** Conceptualization, Methodology, Writing – review & editing, Resources.

Declaration of Competing Interest

There are no conflicts of interest to declare.

Acknowledgments

The authors appreciate the academic support from the Home for Researchers. We also have asked the International Science Editing Corporation to edit the language.

Supplementary materials

Supplementary material associated with this article can be found, in the online version, at doi:10.1016/j.tranon.2022.101562.

References

[1] H. Sung, et al., Global cancer statistics 2020: globocan estimates of incidence and mortality worldwide for 36 cancers in 185 countries, CA Cancer J. Clin. 71 (2021) 209–249, https://doi.org/10.3322/caac.21660.
[2] W.D. Travis, et al., International association for the study of lung cancer/American thoracic society/European respiratory society international multidisciplinary classification of lung adenocarcinoma, J. Thorac. Oncol. 6 (2011) 244–285, https://doi.org/10.1097/JTO.0b013e318206a221.
[3] C. Allemani, et al., Global surveillance of trends in cancer survival 2000-14 (CONCORD-3): analysis of individual records for 37 513 025 patients diagnosed with one of 18 cancers from 322 population-based registries in 71 countries, Lancet 391 (2018) 1023–1075, https://doi.org/10.1016/s0140-6736(17)33326-3.
[4] A. Chaix, A. Zarrinpar, S. Panda, The circadian coordination of cell biology, J. Cell Biol. 215 (2016) 15–25, https://doi.org/10.1083/jcb.201603076.
[5] R.M. Buijs, A. Kalsbeek, Hypothalamic integration of central and peripheral clocks, Nat. Rev. Neurosci. 2 (2001) 521–526, https://doi.org/10.1038/35081582.
[6] F.C. Kelleher, A. Rao, A. Maguire, Circadian molecular clocks and cancer, Cancer Lett. 342 (2014) 9–18, https://doi.org/10.1016/j.canlet.2013.09.040.
[7] H. Dardente, N. Cermakian, Molecular circadian rhythms in central and peripheral clocks in mammals, Chronobiol. Int. 24 (2007) 195–213, https://doi.org/10.1080/07420520701283693.
[8] S. Wang, et al., Upregulation of ARNTL2 is associated with poor survival and immune infiltration in clear cell renal cell carcinoma, Cancer Cell Int. 21 (2021) 341, https://doi.org/10.1186/s12935-021-02046-z.
[9] X. Wang, Y. Li, J. Fu, K. Zhou, T. Wang, ARNTL2 is a prognostic biomarker and correlates with immune cell infiltration in triple-negative breast cancer, Pharmgenom. Pers. Med. 14 (2021) 1425–1440, https://doi.org/10.2147/pgpm.S331431.
[10] M. Lu, et al., ARNTL2 knockdown suppressed the invasion and migration of colon carcinoma: decreased SMOC2-EMT expression through inactivation of PI3K/AKT pathway, Am. J. Transl. Res. 12 (2020) 1293–1308.
[11] N.H. Ha, J. Long, Q. Cai, X.O. Shu, K.W. Hunter, The circadian rhythm gene arntl2 is a metastasis susceptibility gene for estrogen receptor-negative breast cancer, PLos Genet. 12 (2016), e1006267, https://doi.org/10.1371/journal.pgen.1006267.
[12] Z. Tang, et al., GEPIA: a web server for cancer and normal gene expression profiling and interactive analyses, Nucle. Acids Res. 45 (2017) W98–w102, https://doi.org/10.1093/nar/gkx247.
[13] T. Li, et al., TIMER: a web server for comprehensive analysis of tumor-infiltrating immune cells, Cancer Res. 77 (2017) e108–e110, https://doi.org/10.1158/0008-5472.Can-17-0307.
[14] G. Yu, L.G. Wang, Y. Han, Q.Y. He, clusterProfiler: an R package for comparing biological themes among gene clusters, OMICS 16 (2012) 284–287, https://doi.org/10.1089/omi.2011.0118.
[15] A. Mayakonda, D.C. Lin, Y. Assenov, C. Plass, H.P. Koeffler, Maftools: efficient and comprehensive analysis of somatic variants in cancer, Genome Res. 28 (2018) 1747–1756, https://doi.org/10.1101/gr.239244.118.
[16] Z. Liu, et al., Systematic analysis of the aberrances and functional implications of ferroptosis in cancer, iScience 23 (2020), 101302, https://doi.org/10.1016/j.isci.2020.101302.
[17] H. Lian, et al., Integrative analysis of gene expression and DNA methylation through one-class logistic regression machine learning identifies stemness features in medulloblastoma, Mol. Oncol. 13 (2019) 2227–2245, https://doi.org/10.1002/1878-0261.12557.
[18] P. Geeleher, N.J. Cox, R.S. Huang, Clinical drug response can be predicted using baseline gene expression levels and *in vitro* drug sensitivity in cell lines, Genome Biol. 15 (2014) R47, https://doi.org/10.1186/gb-2014-15-3-r47.
[19] F. Finotello, et al., Molecular and pharmacological modulators of the tumor immune contexture revealed by deconvolution of RNA-seq data, Genome Med. 11 (2019) 34, https://doi.org/10.1186/s13073-019-0638-6.
[20] E. Becht, et al., Estimating the population abundance of tissue-infiltrating immune and stromal cell populations using gene expression, Genome Biol. 17 (2016) 218, https://doi.org/10.1186/s13059-016-1070-5.
[21] V. Thorsson, et al., The immune landscape of cancer, Immunity 48 (2018) 812–830, https://doi.org/10.1016/j.immuni.2018.03.023, e814.
[22] Y. Zheng, et al., Multi-omics characterization and validation of MSI-related molecular features across multiple malignancies, Life Sci. 270 (2021), 119081, https://doi.org/10.1016/j.lfs.2021.119081.
[23] H. Yuan, et al., CancerSEA: a cancer single-cell state atlas, Nucleic Acids Res. 47 (2019) D900–D908, https://doi.org/10.1093/nar/gky939.
[24] G.X. Hou, P. Liu, J. Yang, S. Wen, Mining expression and prognosis of topoisomerase isoforms in non-small-cell lung cancer by using Oncomine and Kaplan-Meier plotter, PLoS One 12 (2017), e0174515, https://doi.org/10.1371/journal.pone.0174515.
[25] H. Niu, et al., Knockdown of SMAD3 inhibits the growth and enhances the radiosensitivity of lung adenocarcinoma via p21 *in vitro* and *in vivo*, Int. J. Biol. Sci. 16 (2020) 1010–1022, https://doi.org/10.7150/ijbs.40173.
[26] G. Bi, et al., Knockdown of GTF2E2 inhibits the growth and progression of lung adenocarcinoma via RPS4X *in vitro* and *in vivo*, Cancer Cell Int. 21 (2021) 181, https://doi.org/10.1186/s12935-021-01878-z.
[27] Z. Wang, et al., ARNTL2 promotes pancreatic ductal adenocarcinoma progression through TGF/BETA pathway and is regulated by miR-26a-5p, Cell Death. Dis. 11 (2020) 692, https://doi.org/10.1038/s41419-020-02839-6.
[28] T.A. Chan, et al., Development of tumor mutation burden as an immunotherapy biomarker: utility for the oncology clinic, Ann. Oncol. 30 (2019) 44–56, https://doi.org/10.1093/annonc/mdy495.
[29] T.M. Malta, et al., Machine learning identifies stemness features associated with oncogenic dedifferentiation, Cell 173 (2018) 338–354, https://doi.org/10.1016/j.cell.2018.03.034, e315.
[30] I. Martincorena, P.J. Campbell, Somatic mutation in cancer and normal cells, Science 349 (2015) 1483–1489, https://doi.org/10.1126/science.aab4082.
[31] J. Pan, H. Yang, L. Zhu, Y. Lou, Correlation of ARNTL2 with immune infiltration and its role as a potential prognostic biomarker in lung adenocarcinoma, Clin. Complement. Med. Pharmacol. 1 (2021), https://doi.org/10.1016/j.ccmp.2021.100005.
[32] G. Bi, et al., Identification and validation of tumor environment phenotypes in lung adenocarcinoma by integrative genome-scale analysis, Cancer Immunol. Immunother. 69 (2020) 1293–1305, https://doi.org/10.1007/s00262-020-02546-3.
[33] S. Gery, H.P. Koeffler, Circadian rhythms and cancer, Cell Cycle 9 (2010) 1097–1103, https://doi.org/10.4161/cc.9.6.11046.
[34] J. Gaucher, E. Montellier, P. Sassone-Corsi, Molecular cogs: interplay between circadian clock and cell cycle, Trends Cell Biol. 28 (2018) 368–379, https://doi.org/10.1016/j.tcb.2018.01.006.
[35] T. Matsuo, et al., Control mechanism of the circadian clock for timing of cell division *in vivo*, Science 302 (2003) 255–259, https://doi.org/10.1126/science.1086271.
[36] T.H. Kang, L.A. Lindsey-Boltz, J.T. Reardon, A. Sancar, Circadian control of XPA and excision repair of cisplatin-DNA damage by cryptochrome and HERC2 ubiquitin ligase, Proc. Natl. Acad. Sci. U. S. A. 107 (2010) 4890–4895, https://doi.org/10.1073/pnas.0915085107.
[37] S. Gery, et al., The circadian gene per1 plays an important role in cell growth and DNA damage control in human cancer cells, Mol. Cell 22 (2006) 375–382, https://doi.org/10.1016/j.molcel.2006.03.038.
[38] J.A. Schoenhard, et al., Regulation of the PAI-1 promoter by circadian clock components: differential activation by BMAL1 and BMAL2, J. Mol. Cell Cardiol. 35 (2003) 473–481, https://doi.org/10.1016/s0022-2828(03)00051-8.
[39] T.K. Barbosa Vieira, et al., Correlation between circadian rhythm related genes, type 2 diabetes, and cancer: insights from metanalysis of transcriptomics data, Mol. Cell. Endocrinol. 526 (2021), 111214, https://doi.org/10.1016/j.mce.2021.111214.
[40] G. Mazzoccoli, et al., ARNTL2 and SERPINE1: potential biomarkers for tumor aggressiveness in colorectal cancer, J. Cancer Res. Clin. Oncol. 138 (2012) 501–511, https://doi.org/10.1007/s00432-011-1126-6.
[41] J.J. Brady, et al., An Arntl2-driven secretome enables lung adenocarcinoma metastatic self-sufficiency, Cancer Cell 29 (2016) 697–710, https://doi.org/10.1016/j.ccell.2016.03.003.